

Faint radio–loud quasars: clues to their evolution

M. Cirasuolo, M. Magliocchetti, A. Celotti

S.I.S.S.A., Via Beirut 2-4, I-34014 Trieste, Italy

14 June 2018

ABSTRACT

The quasar sample selected by cross-correlating the FIRST and the 2dF Quasar Redshift Surveys allows us to explore, for the first time, the faint end of the radio and optical luminosity functions up to $z \simeq 2.2$. We find indications ($\sim 3\sigma$) of a negative evolution for these faint sources at $z \gtrsim 1.8$, both in radio and optical bands. This corresponds to a decrement in the space density of faint quasars of about a factor 2 at $z=2.2$ and confirms the presence of a differential evolution for the population of radio-active quasars. The faint end of both luminosity functions flattens and the comparison with the (optical) number density of the whole quasar population supports a dependence of the fraction of radio detected quasars on the optical luminosity. A progressive decrease in the fraction of quasars in the whole radio source population can be consistently accounted for within the ‘receding torus’ scenario. The population of low luminosity quasars, which the FIRST-2dF detects, appears to depart from the ‘classical’ scheme for radio-loud quasars.

Key words: galaxies: active - cosmology: observations - radio continuum: quasars

1 INTRODUCTION

It is becoming increasingly evident that the formation of super-massive black holes (BH) powering nuclear activity is intimately related to the formation of their host galaxies. Observational evidence such as the presence of massive BH ($10^6 - 10^9 M_\odot$) in at least all local galaxies with a spheroidal component (Kormendy & Richstone 1995) and tight correlations between the BH mass and the overall properties of the spheroids supports this connection (Magorrian et al. 1998; McLure & Dunlop 2002; Ferrarese 2002). The evolution of nuclear activity (AGN) with cosmic time is then a key ingredient in order to constrain the formation of galactic systems. Investigations of radio-emitting AGN can be of great help in tackling such issue since – as already proved by very early studies (Longair 1966) – radio emission can be used as a clean tool, not affected by obscuration, to trace the AGN evolution. On the other hand, the connection between the radio and optical activity still needs to be understood.

One of the key studies on the evolution of both radio galaxies and radio quasars, was provided by Dunlop & Peacock (1990). The radio luminosity function (LF) of these populations was separately obtained for steep spectrum and flat spectrum sources, by means of several samples selected at 2.7 GHz with relatively bright flux limits (ranging from 0.1 to 2.0 Jy). This analysis confirmed the presence of a so-called ‘redshift cut-off’ for the population of flat spectrum sources (Peacock 1985), with a decline in comoving density of a factor ~ 5 between $z = 2$ and $z = 4$. Most intriguingly, their work provided the first evidence for a similar behaviour

for the population of steep spectrum sources, both quasars and radio galaxies, making this decline a common feature for all powerful radio objects. The evolution of both populations was found to be satisfactorily described by a pure luminosity evolution (PLE) model, analogous to that found for optically selected quasars (Boyle et al. 1988; Boyle et al. 2000; Croom et al. 2004), as well as by a luminosity/density evolution model, which incorporates a negative density evolution at high redshifts.

In order to investigate the possible presence of a redshift cut-off in the AGN evolution, several searches for high redshift radio-loud quasars have been carried out in the last years. Shaver et al. (1996, 1999) argued for a drop in space density of flat spectrum quasars by more than a factor 10 between $z \sim 2.5$ and $z \sim 6$. However, a re-analysis of such sources (Jarvis & Rawlings 2000; Jarvis et al. 2001) suggests a more gradual (factor ~ 4) decline in the same redshift interval. A luminosity dependent cut-off, with a space density decline less dramatic for the most luminous radio sources, has also been claimed by Dunlop (1998) from a recent update of the work by Dunlop & Peacock (1990).

The question of a redshift cut-off in the quasar evolution has also been addressed at other wavelengths. No evidence for a rapid decline of the quasar space density has been found for soft X-ray selected samples at $z \gtrsim 2.5$ (Miyaji, Hasinger & Schmidt 2000, Ueda et al. 2003). On the other hand, optical data from the Sloan survey (Fan et al. 2001) suggest the space density of $M_{AB}(1450\text{\AA}) < -25.5$ quasars at $z \sim 4$ to be more than one order of magnitude lower than that found at $z \sim 2$ (Boyle et al. 2000). Recently, by using

a sample of 13 optically luminous radio quasars, Vigotti et al. (2003) showed that their decline in the space density is about a factor of 2 between $z \sim 2$ and $z \sim 4$, significantly smaller than the value ~ 10 found for samples including lower luminosity objects (Fan et al. 2001).

However, the comparison with the behaviour of radio-selected sources hinges on the connection between the optical (X-ray) and radio activity. This is clearly of paramount relevance also with regards to the physical connection between the accretion processes and the jet formation. This aspect can be tackled from the comparison of the radio-loud and radio-quiet quasar populations.

The behaviour of radio sources is also tightly connected within the framework of unification models (e.g. Padovani & Urry 1992, Urry & Padovani 1995, Jackson and Wall 1999). These rely on the fact that beaming effects and thus orientation play a key role in determining the observed properties of sources: BL Lac objects and flat spectrum quasars would be the beamed version – i.e. viewed at an angle close to the jet axis – of FRI and FRII radio galaxies (Fanaroff & Riley 1974), respectively. The behaviour of radio quasars is thus closely related to that of the whole radio source population and in particular of powerful radio galaxies.

In the light of the above discussion the aim of the present paper is to estimate the low luminosity end of the LF of radio active quasars, by taking advantage of the new final releases of the 2dF QSO Redshift and the FIRST surveys. The aims are: i) to explore the cosmological evolution of the selected sources, ii) to examine the relation between the radio and optical activity and iii) the connection between quasars and radio galaxies.

The layout of the paper is as follows. In Section 2 we give a brief description of the new final releases of FIRST and 2dF Quasar Redshift Survey datasets used for our analysis and the matching procedure used to cross-correlate the catalogues. In Section 3 we describe the computation of the radio and optical luminosity functions and present our results, giving an assessment for incompleteness effects. Our findings are compared with other LFs already present in literature in Section 4. We discuss the results and summarize our conclusions in Section 5. For sake of comparison with previous works we will adopt $H_0 = 50 \text{ km s}^{-1} \text{ Mpc}^{-1}$, $q_0 = 0.5$ and $\Lambda = 0$ (hereafter cosmology I), but also report our results on both the radio and optical LFs within the “concordance” model, consistent with the Wilkinson Microwave Anisotropy Probe data (Bennett et al. 2003), i.e.: $\Omega_M = 0.3$, $\Omega_\Lambda = 0.7$ and $H_0 = 70 \text{ km s}^{-1}$ (cosmology II).

2 THE DATA SETS

2.1 The FIRST Survey

The FIRST (Faint Images of the Radio Sky at Twenty centimeters) survey (Becker et al. 1995) began in 1993 and its latest release (April 2003), used for this work, contains 811,117 sources observed at 1.4 GHz down to a flux limit $S_{1.4\text{GHz}} \simeq 0.8 \text{ mJy}$. The survey covers a total of about 9033 square degrees of sky (8422 square degrees in the north Galactic cap and 611 in the south Galactic cap) and is substantially complete: it has been estimated to be 95 and 80 per cent complete at 2 mJy and 1 mJy, respectively (Becker

et al. 1995). Note that, as the completeness level quickly drops for flux levels fainter than 2 mJy, in the following analysis we will only consider sources brighter than this limit.

The surface density of objects in the catalogue is ~ 90 per square degree, though this is reduced to $\sim 80 \text{ deg}^{-2}$ if one combines multi-component sources (Magliocchetti et al. 1998). The accuracy of the positions depends both on the brightness and size of the sources and on the noise in the map. Point sources at the detection limit of the catalogue have positions accurate to better than 1 arcsec (90 per cent confidence level); 2 mJy point sources in typically noisy regions have positions determined to better than 0.5 arcsec.

2.2 The 2dF QSO Redshift Survey

The 2dF QSO Redshift Survey (2QZ) has recently been completed and in this work we will refer to the final release (Croom et al. 2004). Here we briefly recall the main properties of the survey. QSO candidates with optical magnitudes $18.25 \leq b_J \leq 20.85$ were selected from the APM catalogue (Irwin, McMahon & Maddox 1994) in two $75^\circ \times 5^\circ$ declination strips centered on $\delta = -30^\circ$ (South Galactic Cap) and $\delta = 0^\circ$ (North Galactic Cap). The following color selection criteria have been applied: $(u - b_j) \leq 0.36$; $(u - b_j) < 0.12 - 0.8(b_j - r)$; $(b_j - r) < 0.05$ (Smith et al. 2003), in order to guarantee a large photometric completeness (> 90 per cent) for quasars within the redshift range $0.3 \leq z \leq 2.2$.

Spectroscopic observations of the input catalogue were made with the 2-degree Field (2dF) instrument at the Anglo-Australian Telescope. The spectra were classified both via cross-correlation with specific templates (AUTOZ, Croom et al. 2004) and by visual inspection.

The final catalogue contains $\sim 21,000$ quasars with reliable spectra and redshift determinations. Whenever available, the 2QZ catalogue also includes radio fluxes at 1.4 GHz from the NRAO VLA Sky Survey (NVSS; Condon et al. 1998) and X-ray fluxes from the ROSAT All Sky Survey (RASS; Voges et al. 1999; Voges et al. 2001).

2.3 Matching Procedure

In order to determine the radio counterparts of 2QZ quasars we have matched objects from the FIRST and 2QZ surveys in the equatorial strip in the North Galactic cap. In the overlapping region $-9^h 50^m \leq \text{RA}(2000) \leq 14^h 50^m$ and $-2.8^\circ \leq \text{Dec}(2000) \leq 2.2^\circ$ – we found 10,110 optical quasars from the 2QZ. Over the same area, the total number of sources in the FIRST survey is $\sim 45,500$ down to a flux limit $S_{1.4\text{GHz}} = 1 \text{ mJy}$. As described in Cirasuolo et al. (2003a; hereafter C03), for the matching procedure we used an algorithm to collapse multi-component sources (Magliocchetti et al. 1998): the algorithm collapses sub-structured sources into single objects having radio fluxes equal to the sum of the fluxes of the various components.

All the optical-radio pairs having an offset less than 2 arcsec have been considered as true optical identifications. The value of 2 arcsec as matching radius was chosen after a careful analysis as the best compromise to maximize the number of real associations (estimated to be ~ 97 per cent), and to minimize the contribution from spurious identifications

down to a negligible 5 per cent (Magliocchetti & Maddox 2002). Furthermore, in order to verify the reliability of the associations, all the radio-optical pairs obtained from the collapsing algorithm were checked by eye on the FIRST image cutouts.

This procedure has lead to 352 quasars with good redshift determinations from the 2QZ and endowed with radio fluxes $S_{1.4\text{GHz}} \geq 1$ mJy over an effective area of 284 square degrees. Of these sources, 113 have been already presented in C03, while the remaining 239 constitute an entirely new sample. The overall sample will be referred to as FIRST-2dF.

As in C03, the reliability of the present sample has also been checked against quasars with a radio counterpart in the NVSS (Condon et al. 1998). The high resolution of FIRST (beaming size 5.4 arcsec) might in fact lead to a systematic underestimate of the real flux density in the case of extended sources. In order to assess the possible presence and entity of this effect, we have then compared FIRST and NVSS (beaming size of 45 arcsec) fluxes for all those sources in the sample which show a radio counterpart in both surveys. In the common 2QZ, FIRST and NVSS region, we only found 253 objects having an NVSS counterpart. All of these sources were also detected by our matching procedure and, as in C03, we found an excellent agreement between fluxes as measured by FIRST and NVSS. No correction to the flux densities derived from the FIRST survey was therefore applied. This also supported the validity of the collapsing algorithm.

About 40 per cent of the sources undetected by NVSS have $S_{1.4\text{GHz}} \geq 3$ mJy, i.e. above the flux limit of the survey (~ 3 mJy). This implies that such objects could have been lost in NVSS because of their multiple component structure.

2.4 Radio spectral index

Radio spectral indices α_R for a sub-sample of FIRST-2dF sources have been obtained by cross-correlating this dataset with the Parkes-MIT-NRAO (PMN) radio survey (Griffith et al. 1995). The PMN survey covers the equatorial zone ($-9.5^\circ \leq \text{Dec}(2000) \leq 10^\circ$), observing objects at 4.85 GHz down to a flux limit of 40 mJy.

Due to its large beaming size, a matching radius of 3 arcmin has been used to cross correlate sources in the PMN with those included in our sample. Out of the 352 objects, we found counterpart for 52 in the PMN catalogue. Note that most of the sources indeed present matching radii ~ 50 arcsec, as shown in the upper panel of Figure 1. Only a few of them have a larger offset, in any case smaller than 2 arcmin. This enables us to be reasonably confident that they are true associations.

The lower panel in Figure 1 shows the distribution of the radio spectral indices obtained. It is clear that the majority of the sources are flat spectrum quasars ($\alpha_R < 0.5$). This is due to the brighter flux limit ($S_{4.85\text{GHz}} = 40$ mJy) of the PMN survey with respect to FIRST. In fact, only bright steep spectrum ($\alpha_R \gtrsim 0.7$) sources with fluxes $S_{1.4\text{GHz}} \gtrsim 100$ mJy could have been detected by PMN, which

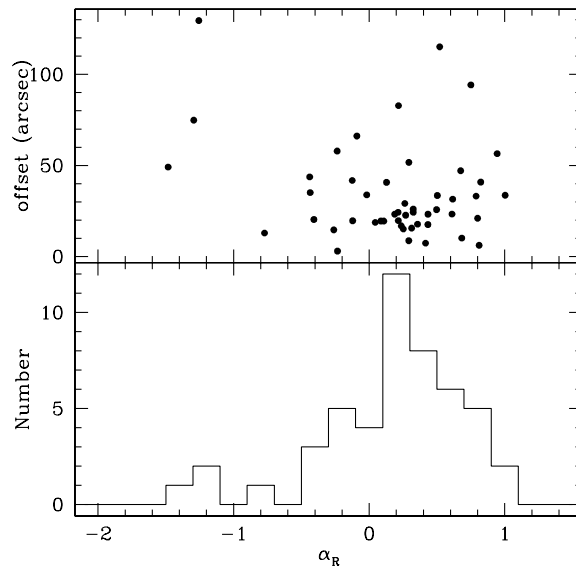


Figure 1. Top panel: radio spectral index for sources in the FIRST-2dF sample versus the offset between the positions in the FIRST and PMN surveys. The lower panel represents the distribution of the radio spectral indices found.

therefore misses the majority of the steep spectrum objects in the FIRST-2dF sample. Out of 49 quasars in the FIRST-2dF sample with $S_{1.4\text{GHz}} \gtrsim 100$ mJy we found 13 steep spectrum and 21 flat spectrum objects. The remaining 15 sources have been missed in the PMN survey due to the fact that it does not cover all of the equatorial region, as it presents holes for $12^h \lesssim \text{RA} \lesssim 16^h$.

2.5 The FIRST-2dF sample

To summarize, the FIRST-2dF sample is comprised of 352 objects with optical magnitudes $18.25 \leq b_J \leq 20.85$ and radio fluxes at 1.4 GHz $S_{1.4\text{GHz}} \geq 1$ mJy. All the 239 objects included in the FIRST-2dF sample and not included in C03 are presented in Table 2.

3 LUMINOSITY FUNCTIONS

The larger size of the present sample with respect to the one presented in C03 (about a factor 3) enables us to obtain the LF of the population of radio detected quasars, both in the radio and optical bands.

In order to minimize incompleteness problems, we only considered sources with $S_{1.4\text{GHz}} > 2$ mJy (i.e. 95 per cent completeness). For the computation of the LFs we further confined the analysis to the redshift range $0.8 < z < 2.2$. The upper limit $z = 2.2$ is due to the drop of completeness at higher redshift of the 2dF QSO Survey (Croom et al. 2004). The choice of $z = 0.8$ as a lower limit is indeed related to the flux limits of both FIRST and 2dF surveys. As shown in Figure 2, faint sources – either in the optical or radio bands – are missed at high redshift due to selection effects. It follows that, in order to have a complete and unbiased coverage of both the $z - M_B$ and $z - P_{1.4\text{GHz}}$ planes only sources with

* Throughout this work the radio flux density is defined as $S_\nu \propto \nu^{-\alpha}$.

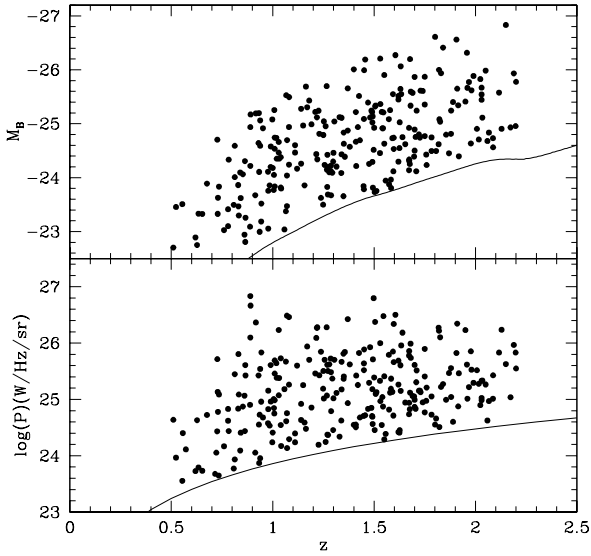


Figure 2. Absolute M_B magnitude (top panel) and radio power at 1.4 GHz (lower panel) versus redshift for sources in FIRST-2dF sample. The solid lines describe the selection effects respectively due to the limiting magnitude $b_J = 20.85$ and radio flux density limit $S_{1.4\text{GHz}} = 2$ mJy.

$M_B \lesssim -24.2$ and $\log_{10} P_{1.4\text{GHz}} \gtrsim 24.5$ ($\text{W Hz}^{-1} \text{sr}^{-1}$) can be considered in the analysis (see Figure 2). In the redshift range $0.5 \lesssim z \lesssim 0.8$ the number of sources satisfying these criteria is extremely small and therefore we considered only sources with $z \geq 0.8$ in the computation of the LFs. After the above corrections, the final sample used for the determination of LFs comprises ~ 200 sources. It is worth noting that in the following analysis photometric and spectroscopic incompleteness of the 2QZ survey in the considered redshift range – both as a function of redshift and apparent magnitude – has been taken into account following Croom et al. (2004).

The radio luminosities at 1.4 GHz have been calculated by using – whenever available – the measured α_R (see Table 2) or adopting a mean value of $\alpha_R = 0.7$ (see Section 2.4).

In order to easily compare our results with those found in the literature we converted magnitudes from the b_J to the B band. The mean $B - b_J$ was computed from the composite quasar spectrum compiled by Brotherton et al. (2001) from ~ 600 radio-selected quasars in the FIRST Bright Quasar Survey (FBQS). Actually in the redshift range $0.3 \leq z \leq 2.2$ the difference between corresponding values in the two bands is very small, $0.05 \lesssim B - b_J \lesssim 0.09$ and independent of redshift. We therefore chose to apply a mean correction $B = 0.07 + b_J$ (see also C03). The K-correction in the B band has also been computed from the Brotherton et al. (2001) composite quasar spectrum.

3.1 Binned $1/V_{\text{max}}$ method

The simplest approach to estimate LFs and their redshift evolution is provided by the ‘classical’ $1/V_{\text{max}}$ method (Schmidt 1968). For each source we evaluated the maximum

redshift at which it could have been included in the sample, $z_{\text{max}} = \min(z_{\text{max}}^R, z_{\text{max}}^O, z_{\text{max}}^S)$, where z_{max}^R and z_{max}^O are the corresponding maximum redshifts due to the radio or the optical limiting flux densities, respectively, and $z_{\text{max}}^S = 2.2$ is the redshift limit of the survey due to completeness.

Radio (RLF) and optical (OLF) luminosity functions have been computed in four equally spaced redshift bins ($\Delta z = 0.35$) and showed in the four panels of Figure 3 and 4, respectively.

3.2 Parametric method

To obtain an independent and more quantitative description of the LFs and to avoid loss of information due to the binning process, we also carried out a maximum likelihood analysis. This is a parametric technique which relies on maximizing the probability of observing exactly one quasar in a $\Delta z \Delta L$ element at each redshift and luminosity for all the quasars in the data set and of observing zero objects in all the other differential elements in the accessible regions of the redshift-luminosity plane (Marshall et al. 1983). This method requires an analytic functional form for the LF and its evolution.

We chose to model both the radio and optical LFs as double power laws in luminosity (or magnitude) as:

$$\Phi(P_{1.4}, z) = \frac{\Phi_0}{(P_{1.4}/P_{1.4}^*)^\alpha + (P_{1.4}/P_{1.4}^*)^\beta} \quad (1)$$

and

$$\Phi(M_B, z) = \frac{\Phi_0}{10^{0.4(1-\alpha)(M_B - M_B^*)} + 10^{0.4(1-\beta)(M_B - M_B^*)}}. \quad (2)$$

The time evolution of the LFs has been modeled with a 2nd-order polynomial function both in the case of pure luminosity evolution:

$$P_{1.4}^*(z) = P_{1.4}^*(z=0) \times 10^{k_1 z + k_2 z^2}, \quad (3)$$

and

$$M_B^*(z) = M_B^*(z=0) - 2.5(k_1 z + k_2 z^2) \quad (4)$$

where $P_{1.4}^*$ and M_B^* are the radio and optical break luminosity, respectively, and pure density evolution:

$$\Phi_0(z) = \Phi_0(z=0) \times 10^{k_1 z + k_2 z^2}. \quad (5)$$

The best fit parameters have been obtained by minimizing the likelihood function, through the MINUIT package from the CERN libraries. The values from the fitting are given in Table 1 for both the radio and optical LFs. Errors on each parameter, corresponding to 68 per cent confidence level, have been obtained by using the MINOS task in MINUIT. The algorithm procedure consists in varying one parameter at a time, and then minimizing the likelihood function with respect to all the other parameters, in order to find the variation in the function corresponding to one standard deviation error. Figures 3 and 4 show the best-fit solutions obtained from the likelihood analysis (solid curves), compared with the LFs obtained with the binned method (Section 3.1). The analytic functions have been computed at the mean redshift of each bin. The agreement between the LFs obtained through these two independent methods is remarkably good.

To have a quantitative assessment of the goodness of

Radio LF								
Cosmology	Evol.	α	β	$\log_{10} P_{1.4}^*$	k_1	k_2	Φ_0	P_{KS}
I	L	-0.1 ± 0.1	1.5 ± 0.2	22.7 ± 0.4	4.5 ± 0.5	-1.5 ± 0.2	5.0×10^{-8}	0.2
I	D	-0.1 ± 0.1	1.6 ± 0.3	26.0 ± 0.2	2.9 ± 0.6	-0.9 ± 0.2	2.5×10^{-10}	0.6
II	L	-0.1 ± 0.1	1.5 ± 0.2	22.9 ± 0.5	4.3 ± 0.6	-1.5 ± 0.2	4.2×10^{-8}	0.2
II	D	-0.1 ± 0.1	1.7 ± 0.4	26.0 ± 0.2	2.9 ± 0.6	-0.9 ± 0.2	2.0×10^{-10}	0.5

Optical LF								
Cosmology	Evol.	α	β	M^*	k_1	k_2	Φ_0	P_{KS}
I	L	0.2 ± 0.6	2.4 ± 0.5	20.4 ± 1.0	2.3 ± 0.5	-0.8 ± 0.2	6.3×10^{-8}	0.6
I	D	0.7 ± 0.2	2.9 ± 0.7	25.6 ± 0.4	1.3 ± 0.5	-0.5 ± 0.1	5.3×10^{-9}	0.5
II	L	0.6 ± 0.3	2.8 ± 0.3	21.1 ± 1.0	2.0 ± 0.5	-0.6 ± 0.2	4.4×10^{-8}	0.4
II	D	0.8 ± 0.2	2.8 ± 0.7	25.6 ± 0.5	1.4 ± 0.5	-0.5 ± 0.2	3.1×10^{-9}	0.5

Table 1. Best fit parameters for the radio and optical LF of the FIRST-2dF sample. The characters L and D in the second column refer to a model of luminosity (Eq. 3) or density (Eq. 5) evolution, respectively.

the best-fit parameters we used a 2D Kolmogorov-Smirnov (KS). This multidimensional version of the KS test (Press et al. 1992) compares the observed redshift-luminosity plane with the one obtained integrating the LF. Note that the KS test can only be used to reject models when the resulting probability P_{KS} is less than 0.1 or 0.05. In our case the probability P_{KS} values are ≥ 0.2 (see Table 1), implying that the data and model are not significantly different.

Note that in the considered redshift range ($0.8 \lesssim z \lesssim 2.2$) the radio LFs obtained with the two evolution models are very similar, since we are sampling only the faint end of the LF. Figures 3 and 4 show the results for the luminosity evolution model. In order to provide a more direct visualization of the redshift evolution of the LFs, in each panel of Figures 3 and 4 we also reported – as a dotted line – the LF at the maximum of its redshift evolution which is reached in both the radio and optical bands at $z \sim 1.7 \pm 0.2$. We note that this preliminary analysis suggests the presence of a decline in the observed number density of objects at $z \sim 2$. Even though this decline is not statistically significant and more data are needed to verify the trend, this appears to hold in both bands. We will present stronger evidence for such a finding in Section 4.

3.3 Assessment of incompleteness

It is worth noting that the LFs presented in the previous Section have been computed by applying various cuts to the dataset, both in redshift and luminosity. In fact, the analysis has been confined to a particular redshift range ($0.8 \leq z \leq 2.2$). Moreover, limits have been applied to both radio and optical luminosities, in order to avoid incompleteness effects and obtain an unbiased coverage of the redshift-luminosity planes. In this section we try to estimate the effects of these limits on the derived LFs, with particular attention devoted to the $M_B \lesssim -24.2$ and $\log_{10} P_{1.4\text{GHz}} \gtrsim 24.5$ ($\text{W Hz}^{-1} \text{sr}^{-1}$) cuts.

In order to provide an estimate of the incompleteness affecting the radio LF, we considered the redshift interval $0.5 \lesssim z \lesssim 1.2$, in which the coverage of the $z - M_B$ plane

is complete down to $M_B \sim -23$ (see Figure 2). In this redshift range, we computed the RLF applying either a cut at $M_B \leq -24.2$ or $M_B \leq -23$. It turns out that the shape of the RLF does not change by applying these two limits, while the normalization obtained in the case of $M_B \leq -24.2$ is about 2 times lower than that found in the $M_B \leq -23$ case. We stress that due to the small statistics in this redshift range such result should only be taken as a rough estimate of the true incompleteness. Therefore, under the “strong” assumption that the $M_B \leq -24.2$ cut only affects the normalization of the RLF, independently of redshift, we can correct the RLF by a factor 2 in normalization, in order to have a rough estimate of the “complete” RLF of quasars down to $M_B \leq -23$.

We also tested for the effects of the $\log_{10} P_{1.4\text{GHz}} \geq 24.5$ ($\text{W Hz}^{-1} \text{sr}^{-1}$) cut on the OLF. In the same redshift range ($0.5 \lesssim z \lesssim 1.2$) we can achieve completeness down to $\log_{10} P_{1.4\text{GHz}} \geq 24$ (see bottom panel of Figure 2). An analysis analogous to that applied for the RLF reveals that the cut at $\log_{10} P_{1.4\text{GHz}} \geq 24.5$ ($\text{W Hz}^{-1} \text{sr}^{-1}$) does not affect the shape of OLF, as in the case of the RLF, but only its normalization by a factor ~ 1.5 . Both radio and optical LFs corrected for this incompleteness, assumed to hold at all redshifts (i.e. for LFs with a shape independent of z), are shown as dot-dashed lines in Figures 3 and 4.

4 COMPARISON WITH PREVIOUS RESULTS

4.1 Radio Luminosity Function

Our results on the RLF can be meaningfully compared at its bright end with those obtained for bright radio selected quasars by Willott et al. (1998). A sample of steep spectrum quasars with $M_B < -23$ was selected by these authors from the 7C (McGilchrist et al. 1990) and 3CRR (Laing et al. 1983) catalogues. All their sources are found to be radio loud, due to the bright limits of these low frequency surveys, $S_{151\text{MHz}} \geq 0.51$ Jy and $S_{178\text{MHz}} \geq 10.9$ Jy, respectively.

Before moving on, a caveat is necessary. Our dataset cannot discriminate between steep and flat objects. As dis-

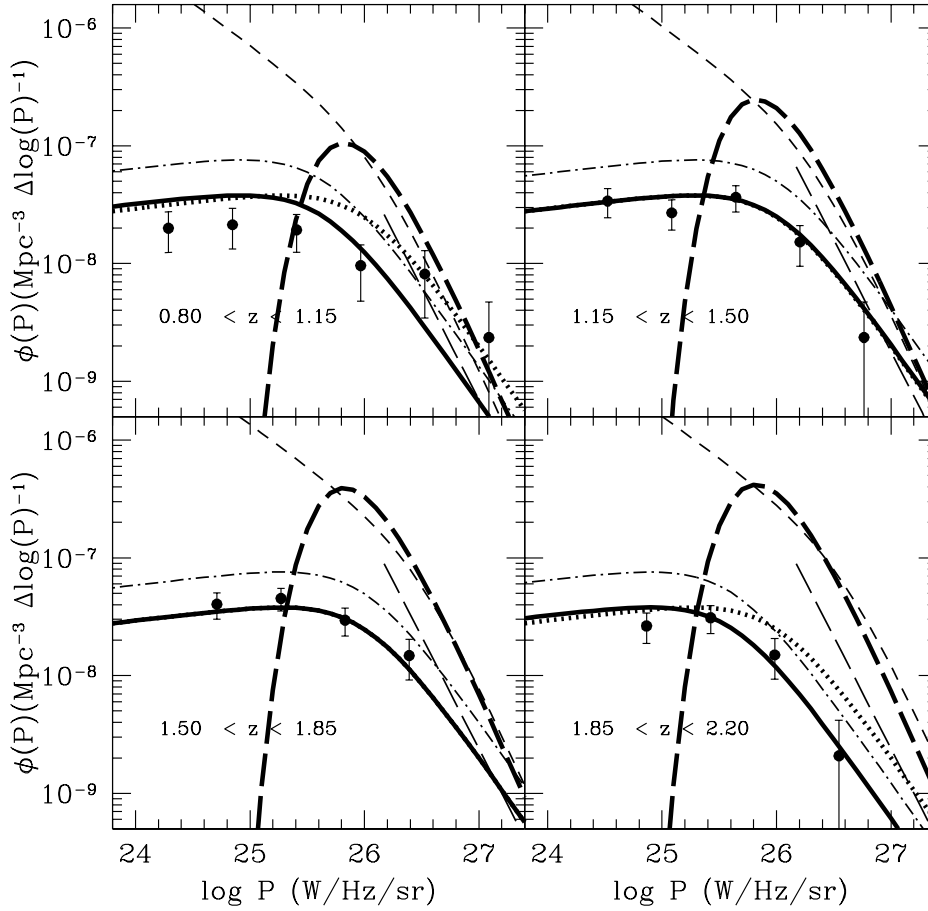


Figure 3. Radio luminosity functions for sources in the FIRST-2dF sample. The filled circles represent the LF obtained with the $1/V_{\max}$ method and the solid lines those derived from the likelihood analysis, by assuming a luminosity evolution model in cosmology I. The dotted lines indicate the RLF at the redshift of its maximum, while the dot-dashed lines are the RLFs corrected in normalization by a factor of 2 (see text). For comparison, we also plotted the LFs from Dunlop & Peacock (1990) (dashed), Willott et al. (1998) for steep spectrum radio loud quasars (thin long-dashed lines) and Willott et al. (2001) for the high luminosity radio population (thick long-dashed lines).

cussed in Section 2.4, most of the sources in the FIRST-2dF sample are probably steep spectrum, as suggested by the lack of detection in the PMN. Moreover, at low radio powers ($\log_{10} P_{1.4\text{GHz}} \lesssim 26 \text{ W Hz}^{-1} \text{ sr}^{-1}$), the number of flat spectrum sources is much smaller than the steep spectrum ones even in samples selected at high frequencies (Dunlop & Peacock 1990; Maraschi & Rovetti 1994). Therefore, this allows us to directly compare our data with the steep spectrum dataset of Willott et al. (1998).

In order to perform this comparison, we have converted source luminosities from the Willott et al. (1998) sample to 1.4 GHz by assuming a radio spectral index $\alpha_R = 0.7$. The RLF for their best fit (model C) are shown in Figure 3 as thin long dashed lines.

These appear to be in reasonably good agreement with our RLF (corrected for renormalization, see Section 3.3). In fact, the slopes of the bright ends are similar, even though the statistics of our data is very poor in this luminosity range. Our best fit value for the slope is 1.7 ± 0.3 , fully con-

sistent with 1.9 ± 0.1 quoted by Willott et al. (1998). The second important aspect is related to the flattening of the RLF at the faint end. Due to the paucity of data, Willott et al. estimated the value of the break luminosity by fixing a slope $\alpha = 0$ for the faint end and fitting the radio number counts at 0.1 Jy. This procedure led to a value of the break luminosity $\log_{10} P_{151\text{MHz}}^* \sim 26.8 \text{ (W Hz}^{-1} \text{ sr}^{-1})$, i.e. ~ 26.0 when translated at 1.4 GHz. With our sample – which is more than 100 times fainter than the 7C – we can directly determine for the first time this flattening and our analysis confirms that the faint end is well described by $\alpha \sim 0$. Furthermore, we infer a break at a luminosity $\log_{10} P_{1.4\text{GHz}} \sim 26 \text{ W Hz}^{-1} \text{ sr}^{-1}$ in agreement with that deduced by Willott et al. (1998), by considering both a luminosity and a density evolution model.

The evolution of the RLF found in our sample is also consistent with that derived for brighter sources, showing a maximum at $z \sim 1.7$. However, the FIRST-2dF sample shows indications for negative evolution beyond $z \sim 1.8$ (see

Section 3.2), while the brighter Willott et al. sample is consistent with no evolution up to the highest redshifts probed by their surveys ($z \sim 3$). However, their statistics in the $2 \lesssim z \lesssim 3$ range is rather limited (< 10 sources).

In order to assess the significance of our finding of a negative evolution beyond $z \sim 1.8$, we considered the behaviour of the quasar number density $\rho(z)$ as a function of redshift. This is obtained by integrating the LFs over the luminosity range detectable up to the highest redshift in our data. It is worth noting that, even though we do not have information on the bright end of the RLF, our sample extends up to the break of the LF, thus accounting for the bulk of the sources. The number density $\rho(z)$ is plotted in Figure 5, where the error bars indicate Poissonian uncertainties. We find that the space density of FIRST-2dF quasars shows a significant ($\sim 3\sigma$) tendency for a decrement at $z \gtrsim 1.8$. Such a decrement is found to be approximately a factor 2 at $z = 2.2$. These results hold in both cosmologies. In the small panel of Figure 5 we also show the space density computed for two bins of radio power. The decline observed for the whole sample is still evident for low-luminosity objects as well as for brighter ones. For the latter sources the decline seems to be less pronounced, but the small statistics does not allow to draw any conclusion.

We note that our choice of adopting a single spectral index ($\alpha_R = 0.7$) for all the sources undetected by PMN could introduce some uncertainties in the determination of $\rho(z)$. In fact, radio spectra steepen at higher frequencies and, as shown by Jarvis & Rawlings (2000), this is crucial in determining the space density of radio objects at high redshift. In order to quantify this uncertainty we have then considered an “extreme case” by assuming for all the sources with $z > 1.7$ a steep spectral index ($\alpha_R = 1.5$). Clearly this results in larger radio powers and in turn in a rise in the bright end of the LF, to the detriment at fainter luminosities. The crucial point is to assess the completeness of the sample. In fact, due to the steeper spectral index at high z , the observed fluxes would drop more rapidly with redshift. However, even by assuming such a steep spectral index ($\alpha_R = 1.5$) for $z > 1.7$, the 2 mJy limit of our sample ensures completeness down to $\log_{10} P_{1.4\text{GHz}} \sim 25 \text{ W Hz}^{-1} \text{ sr}^{-1}$ for $z \leq 2.2$. This, together with the fact that the trend for the space density of fainter and brighter sources is found to be similar (see Figure 4), makes us confident that our results, and particularly those on the space density of radio-loud quasars, are not severely affected by the uncertainty associated to an unknown spectral index.

Another source of uncertainty could arise from the double selection, radio and optical, of the sample since radio and optical luminosities are related, even though with a large scatter (Cirasuolo et al. 2003b). Therefore, low luminosity radio sources would be affected by the optical flux limit more quickly than the brighter ones. This selection effect would be effective at all redshifts, but stronger at high z due to the redshift dependence of the limiting luminosity (see Figure 2), producing a fake decline in the space density. However, the large scatter between radio and optical luminosities – at least three orders of magnitude in radio luminosity at a fixed optical one (Cirasuolo et al. 2003a) – completely dominates over this selection effect. This is again supported by the similar decline in space density at high redshift of sources with different radio powers (see Figure 5).

The last point worth stressing is that we find no evidence for a strong decrement in the space density at low redshifts. In fact, $\rho(z)$ is found to decrease by only a factor ~ 1.5 between $z \sim 1$ and $z \sim 0.5$. This lack of a significant evolution at low redshifts has also been recently claimed by Clewley & Jarvis (2004) for fainter sources ($P_{325\text{MHz}} < 10^{25} \text{ W Hz}^{-1} \text{ sr}^{-1}$) at $z < 0.5$, even though the evolution of the very low luminosity population (i.e. FR I) still remains unconstrained (Magliocchetti, Celotti & Danese 2002).

4.2 Optical Luminosity Function

Clearly the best reference for the OLF of the radio quasar sample is constituted by the OLF of the ‘parent’ (2dF QSO Redshift Survey) population (Croom et al. 2004).

In Figure 4 we report the best fit solutions for the OLF found by Croom et al. (2004) (dashed lines, corresponding to the polynomial evolution model in the case of cosmology I). As in the case of the RLF, we applied a correction of a factor 1.5 in the normalization of our OLF to account for incompleteness effects (see Section 3.3). This provides an estimate of the OLF (dot-dashed lines) representative of the whole population of radio-active quasars with $\log_{10} P_{1.4\text{GHz}} \geq 24 \text{ (W Hz}^{-1} \text{ sr}^{-1})$.

As expected, the OLF of radio detected quasars is flatter than the one derived for the population as a whole. This is already visible at the brighter end where the slope of the FIRST-2dF OLF is $\beta \sim 2.4 - 2.8$ (depending on the adopted model), while that obtained by Croom et al. (2004) is $\beta = 3.2$. This trend becomes increasingly more significant towards fainter magnitudes. Indeed, this is consistent with the observed dependence of the fraction of radio detected quasars as a function of optical luminosity (Padovani 1993; La Franca et al. 1994; Hooper et al. 1995; C03). However, Cirasuolo et al. (2003b) showed that this can simply be the result of selection effects due to the radio and optical limits of the various samples, under the assumption that the optical and radio luminosities are linearly (even though) broadly correlated. In this case the intrinsic shape of the distribution of the radio-to-optical ratio $R_{1.4\text{GHz}}^*$ for the quasar population as a whole is found to show a broad peak at $R_{1.4\text{GHz}}^* \sim 0.3$ containing more than 90 per cent of the sources, followed by a steep transition region at $1 \lesssim R_{1.4\text{GHz}}^* \lesssim 10$ (see Fig. 4 in Cirasuolo et al. 2003b). This implies that, at a given radio flux limit, surveys with brighter optical limiting magnitudes preferentially select smaller values of $R_{1.4\text{GHz}}^*$ – i.e. closer to the peak of the distribution – which results in a higher percentage of radio detections.

In Figure 4 we also compare our results with previous determinations of the OLF for bright ($M_B \lesssim -25$) radio-loud quasars (La Franca et al. 1994; their best-fit function (model B) is indicated with long-dashed lines). An overall good agreement between the two OLFs is found in the magnitude range in which the two samples overlap.

The OLF obtained from our sample peaks at $z \sim 1.7$ and – as in the case of the RLF – possibly hints to a decline at higher redshifts. On the contrary, La Franca et al. (1994) find a maximum redshift for luminosity evolution $z_{\text{max}} \sim 1.9$, beyond which no further evolution is detected. The same substantial lack of evolution in the range $1.5 \lesssim z \lesssim 2$ has also been claimed by Goldschmidt et al.

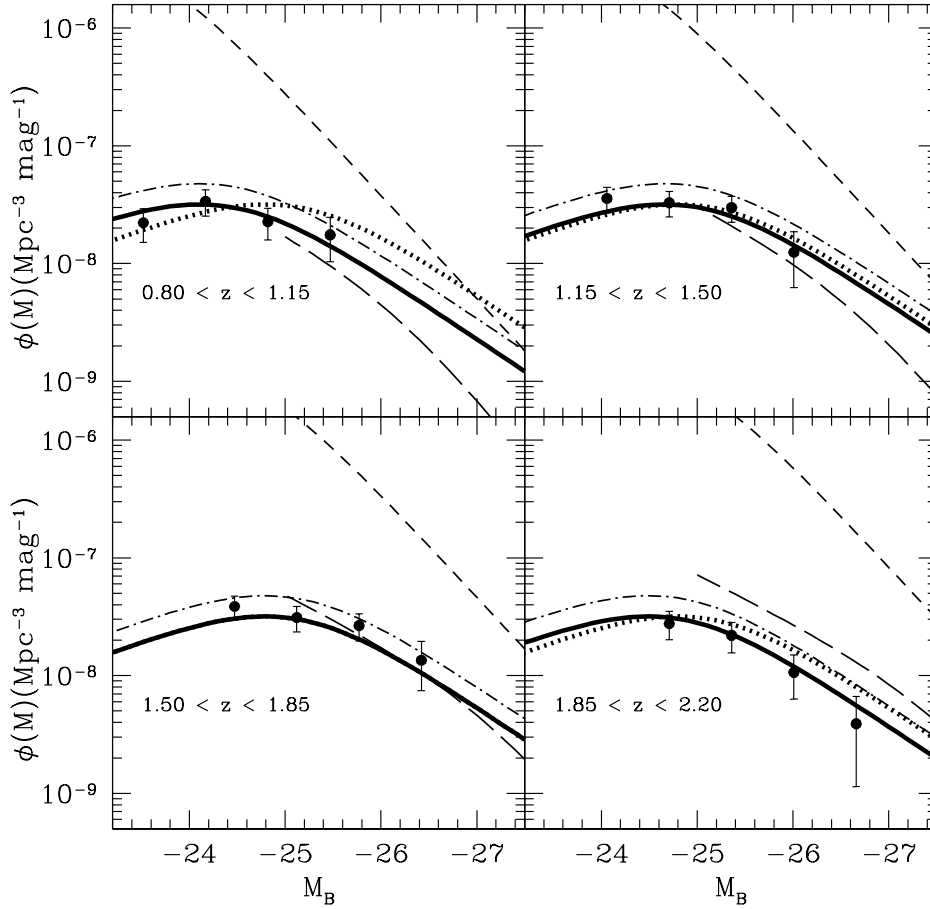


Figure 4. Optical luminosity functions for sources in the FIRST-2dF sample. The filled circles represent the LF obtained with the $1/V_{\max}$ method and the solid lines those derived from the likelihood analysis, by assuming a luminosity evolution model in cosmology I. The dotted lines indicate the OLF at the redshift of its maximum, while the dot-dashed lines are the OLFs corrected in normalization by a factor of 1.5 (see text). For comparison, we also plotted the LFs from La Franca et al. (1994) (long-dashed) and for the quasar population as a whole (Croom et al. 2004, dashed lines).

(1999). However, we argue that the limited sizes of their $z \sim 2$ samples do not allow for any strong statistical conclusion.

4.3 The whole radio source population

Let us finally consider the relation between the radio quasar and the entire radio source population. The dashed lines in Figure 3 represent the RLF for steep plus flat spectrum radio sources obtained by Dunlop & Peacock (1990) (calculated at 1.4 GHz by assuming a radio spectral index $\alpha_R = 0.7$ for steep spectrum sources). It is clear that the fraction of radio quasars decreases toward lower powers, implying that for $\log_{10} P_{1.4\text{GHz}} \lesssim 26$ ($\text{W Hz}^{-1} \text{sr}^{-1}$) the fraction of radio galaxies is dominant with respect to radio quasars, while at higher luminosities the two populations are of comparable importance. The shaded area in Figure 6 shows the ratio f_{QSO} between the RLF of radio quasars – drawn from the FIRST-2dF sample and corrected in normalization – and the RLF of Dunlop & Peacock (1990) as a func-

tion of radio luminosity. The increasingly larger scatter for $\log_{10} P_{1.4\text{GHz}} \gtrsim 25.5$ ($\text{W Hz}^{-1} \text{sr}^{-1}$) is due to the different evolution in redshift of the two RLFs. As already discussed, the space density of radio active quasars is found to decline at high redshift, while the radio population as a whole still shows a positive evolution, therefore increasing the scatter in f_{QSO} . A similar trend in the fraction of quasars as a function of luminosity has been found by Willott et al. (2000) by analyzing radio selected samples. They found that this fraction is ~ 40 per cent at bright (narrow [OII]) emission line luminosities ($L_{[\text{OII}]}$) – assumed to be good tracer of the ionizing continuum – dropping to a few per cent for fainter luminosities. They suggested that this finding can be accounted for by either a gradual decrease of the opening angle of the obscuring ‘torus’ with decreasing ionizing luminosity or with the emergence of a distinct population of low luminosity radio sources, M87-like.

Following the approach suggested by Willott et al. (2000) we try to interpret the decrease of f_{QSO} within the ‘receding torus’ scenario. In this model, initially proposed

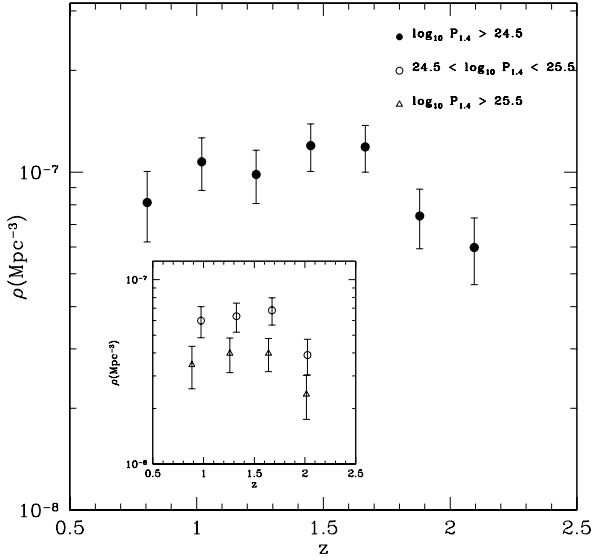


Figure 5. Space density as a function of redshift for sources in the FIRST-2dF sample for cosmology I. The small panel shows the same space density for two different bins in radio power.

by Lawrence (1991; see also Simpson 1998), the inner radius of the torus depends on the AGN radiation field which sublimates the dust grains. If the scale-height of the torus is independent of the ionizing luminosity L_{ion} , its inner radius scales as $L_{\text{ion}}^{0.5}$ resulting in larger half-opening angles θ at higher luminosities. The fraction of quasars predicted is then:

$$f_{\text{QSO}} = 1 - \left(1 + \left(\frac{L_{\text{ion}}}{L_0}\right) \tan^2 \theta_0\right)^{-0.5}, \quad (6)$$

where L_0 and θ_0 are a normalization luminosity and the corresponding torus half-opening angle, fixed by the measured quasar fraction at that luminosity. As we cannot rely on the $L_{[\text{OII}]}$ as Willott et al., as a working hypothesis we use the radio luminosity as a tracer of the central ionizing radiation field. This is based on the linear relation between radio power at 151 MHz and $L_{[\text{OII}]}$ suggested by Willott (2000), $L_{[\text{OII}]} \propto L_{151}^{1.0}$, although with a large scatter (see also Willott et al. 1999). Because of this uncertainty, we modified Eq. 6 assuming that the ionizing luminosity scales as P^δ , where P is the radio power at 1.4 GHz and δ is a free parameter, i.e.:

$$f_{\text{QSO}} = 1 - \left(1 + \left(\frac{P}{P_0}\right)^\delta \tan^2 \theta_0\right)^{-0.5}. \quad (7)$$

Different values for the parameter δ have been tested in order to reproduce the measured fraction of radio active quasars. As shown in Figure 6, a nearly linear dependence of the central ionizing luminosity on the radio power ($\delta \sim 1$) is able to reproduce the observed fraction, $\delta \simeq 0.5$ is only marginally consistent with it, while the extreme value $\delta = 2$ is totally inconsistent with the observed behaviour. This finding is a posteriori broadly consistent with the relation $L_{[\text{OII}]}$ vs L_{151} found by Willott (2000) and with the evidence found by Cirasuolo et al. (2003b) for a nearly linear dependence of the radio luminosity on the optical one.

However, the linear relation used in Eq. (7) does not

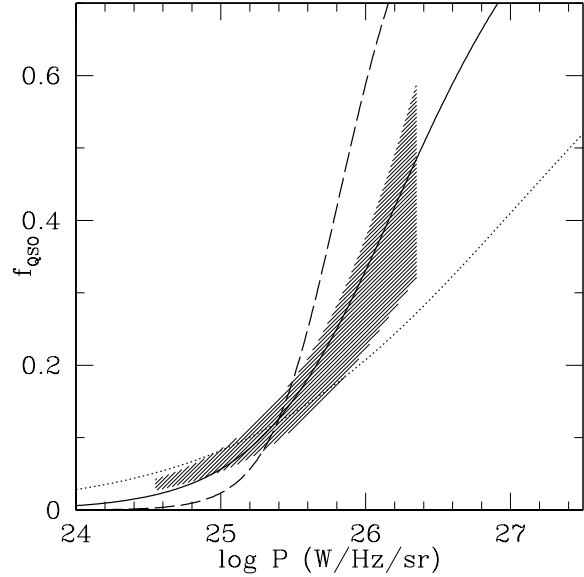


Figure 6. Fraction f_{QSO} of radio quasars from the FIRST-2dF sample with respect to the whole radio population (taken from Dunlop & Peacock 1990) as a function of radio power (shaded area). The solid line is the predicted fraction on the basis of equation 7 assuming $\delta = 1$, while the dotted and dashed lines respectively correspond to $\delta = 0.5$ and $\delta = 2$. The predicted fractions have been normalized at $\log_{10} P_{1.4\text{GHz}} = 25.5 \text{ W Hz}^{-1} \text{ sr}^{-1}$.

take into account the large scatter between radio and optical/UV luminosities, which could mask the effect postulated by the receding torus model. An observational way to test whether indeed $\gtrsim 90\%$ of weak radio sources contain a hidden quasar – as implied by such model – would be the measure of the level of their nuclear (disc/torus) activity through far-IR photometry (i.e. with SPITZER).

The comparison between the radio quasar and the whole radio source population within the framework of the unification scenario – postulating that radio-loud quasars represent the beamed counterparts of powerful (FR II) radio sources – reveals a further aspect worth mentioning. Willott et al. (2001) proposed a dual population model for the RLF by separating the contribution from the high and low luminosity sources assumed to have a differential density evolution. The latter population can be associated with weak/low ionization emission lines radio galaxies – both FR I and FR II – while the high luminosity population can be representative of radio galaxies and quasars with strong/high ionization emission lines and FR II radio properties. A comparison of our RLF with that of the high power population identified by Willott et al. (2001) (converted to 1.4 GHz by assuming $\alpha_R = 0.7$; thick long-dashed lines in Figure 3) shows that at $\log_{10} P_{1.4\text{GHz}} < 25 \text{ (W Hz}^{-1} \text{ sr}^{-1})$ the observed quasar number density largely exceeds that of the whole population [†] as derived by Willott et al.

[†] Formally, the low luminosity end of the distribution of the Willott et al. (2001) powerful population actually cuts even above the definition of FR II-like sources ($\log_{10} P_{1.4\text{GHz}} \sim 24.5 \text{ W Hz}^{-1} \text{ sr}^{-1}$ at 1.4 GHz).

It is worth reminding here that all of the sources in the FIRST-2dF sample are classified as quasars, based on both their broad emission lines and bright luminosity ($M_B \leq -23$). Furthermore, they are radio loud according both to their radio luminosity ($\log_{10} P_{1.4\text{GHz}} \geq 24 \text{ W Hz}^{-1} \text{ sr}^{-1}$; Miller et al. 1990) and radio-to-optical ratio ($R_{1.4\text{GHz}}^* \geq 30$; Kellermann et al. 1989). However, for the first time, the FIRST-2dF sample is able to explore the low optical and radio luminosity ranges. In particular, the radio powers sampled with this work approach the transition region between FRII and FRI sources, posing the problem of the nature of these low luminosity objects.

A few possibilities are open. They could hint at a population of quasars with intermediate FRII-FRI radio properties, either intrinsic or due to an evolution between these two radio phases (such as those discussed by Blundell & Rawlings 2001). Alternatively, these objects might be bordering the intermediate radio quasar population (i.e. between loud and quiet radio quasars with no evidence for relativistic jets). Finally, they might simply represent a lower luminosity version of powerful radio quasars, which thus do not obviously fit into the ‘classical’ scheme for radio sources. This might correspond to the fading phase of luminous quasars. Interesting clues on this issue would come from the study of their radio morphology.

5 DISCUSSION

The novelty of our work is that, by exploiting the faint observational limits of both radio and optical surveys such as the FIRST and the 2dF Quasar Redshift Survey, it was possible for the first time to explore the faint end of the LFs of radio (loud) quasars at both wavelengths. Furthermore, the larger number of radio-detected quasars collected by using these datasets allowed for a suitable determination of these LFs up to $z \sim 2.2$.

The most intriguing result we found is the indication ($\sim 3\sigma$) – both in radio and optical band – of a negative evolution for these faint sources at $z > 1.8$. This corresponds to a decrement in the space density of faint quasars of about a factor 2 at $z \simeq 2.2$. For brighter – either radio or optically selected – samples, the evolution of radio-loud quasars shows a peak at $z \sim 1.7 - 2.0$, but no evidence for a decline at higher redshifts (Willott et al. 1998; La Franca et al. 1994; Goldschmidt et al. 1999). This result is thus consistent with the presence of a differential evolution for the population of radio-active quasars (Vigotti et al. 2003), where the weakest radio sources show a more pronounced decline in space density than the more powerful ones, suggesting the evolution to be a function of the intrinsic power (as in the luminosity/density evolution model of Dunlop & Peacock 1990).

The second interesting finding is the flattening of the faint end of the LFs of radio active quasars in both the radio and optical bands. The found behaviour of the OLF at faint magnitudes is consistent with previous estimates performed at brighter magnitudes (La Franca et al. 1994; Goldschmidt et al. 1999), and the comparison with the OLF of the quasar population as a whole supports a dependence of the fraction of radio detected quasars on their optical luminosity. This flattening can simply result from a linear although broad intrinsic correlation between the radio and optical luminosities

when combined with the radio and optical limits of the various surveys (Cirasuolo et al. 2003b).

Finally, we find that a progressive decrement in the fraction of quasars in the whole radio source population can be consistently accounted for within the ‘receding torus’ scenario by assuming a quasi-linear dependence between optical and radio luminosities. At this stage, the nature of the lower radio luminosity sources in our sample appears unclear substantially due to the lack of information on the origin/characteristics of their radio emission, which could be unveiled by higher resolution radio imaging.

6 ACKNOWLEDGMENTS

We wish to thank Luigi Danese for insightful discussions and the referee for helpful comments. We also acknowledge J.A. Peacock and G. Zamorani for useful suggestions. The Italian MIUR and INAF are acknowledged for financial support.

REFERENCES

- Becker R.H., White R.L., Helfand D.J., 1995, *ApJ*, 450, 559
- Bennett C.L., et al. 2003, *ApJ*, 583, 1
- Blundell K.M., Rawlings S., 2001, *ApJ*, 562, 5
- Boyle B.J., Shanks T., Peterson B.A., 1988, *MNRAS*, 235, 935
- Boyle B.J., Shanks T., Croom S.M., Smith R.J., Miller L., Loaring N., Heymans C., 2000, *MNRAS*, 317, 1014
- Brotherton M.S., Tran H.D., Becker R.H., Gregg M.D., Laurent-Muehleisen S.A., White R.L., 2001, *ApJ*, 546, 775
- Cirasuolo M., Magliocchetti M., Celotti A., Danese L., 2003a, *MNRAS*, 341, 993 (C03)
- Cirasuolo M., Celotti A., Magliocchetti M., Danese L., 2003b, *MNRAS*, 346, 447
- Clewley L., Jarvis M.J., 2004, *MNRAS*, 352, 909
- Condon J.J., Cotton W.D., Greisen E. W., Yin Q.F., Perley R.A., Taylor G.B., Broderick J.J., 1998, *AJ*, 115, 1693
- Croom S.M., Smith R.J., Boyle B.J., Shanks T., Loaring N.S., Miller L., Lewis I.J., 2001, *MNRAS*, 322, L29
- Croom S.M., Schade D., Boyle B.J., Shanks T., Miller L., Smith R.J., 2004, *ApJ*, 606, 126
- Dunlop J.S., Peacock J.A., 1990, *MNRAS*, 247, 19
- Dunlop J.S., 1998, in Bremer M.N., et al., eds., *Observational Cosmology with the New Radio Surveys*. Kluwer
- Fan X., et al. 2001, *AJ*, 121, 54
- Fanaroff B.L., Riley J.M., 1974, *MNRAS*, 167, 31
- Ferrarese L., 2002, *ApJ*, 578, 90
- Griffith M.R., Wright A.E., Burke B., Ekers R.D., 1995, *ApJS*, 97, 347
- Goldschmidt P., Kukula M.J., Miller L., Dunlop J.S., 1999, *ApJ*, 511, 612
- Hooper E.J., Impey C.D., Foltz C.B., Hewett P.C., 1995, *ApJ*, 445, 62
- Irwin M.J., McMahon R.G., Maddox S.J., 1994, *Spectrum*, 2, 14
- Jackson C.A., Wall J.V., 1999, *MNRAS*, 304, 160
- Jarvis M.J., Rawlings S., 2000, *MNRAS*, 319, 121
- Jarvis M.J., Rawlings S., Willott C.J., Blundell K.M., Eales S., Lacy M., 2001, *MNRAS*, 327, 907
- Kellermann K.I., Sramek R., Schmidt M., Shaffer D.B., Green R., 1989, *AJ*, 98, 1195
- Kormendy J., Richstone D., 1995, *ARA&A*, 33, 581
- La Franca F., Gregorini L., Cristiani S., De Ruiter H., Owen F., 1994, *AJ*, 108, 1548
- Laing R.A., Riley J.M., Longair M.S., 1983, *MNRAS*, 204, 151
- Lawrence A., 1991, *MNRAS*, 252, 586

- Longair M.S., 1966, MNRAS, 133, 421
- Magliocchetti M., Maddox S.J., Lahav O., Wall J.V., 1998, MNRAS, 300, 257
- Magliocchetti M., Maddox S.J., 2002, MNRAS, 330, 241
- Magliocchetti M., Celotti A., Danese L., 2002, MNRAS, 329, 377
- Magorrian J., et al., 1998, AJ, 115, 2285
- Maraschi L., Rovetti F., 1994, ApJ, 436, 79
- Marshall H.L., Tananbaum H., Avni Y., Zamorani G., 1983, ApJ, 269, 35
- McGilchrist M.M., Baldwin J.E., Riley J.M., Titterton D.J., Waldrum E.M., Warner P.J., 1990, MNRAS, 249, 110
- McLure R.J., Dunlop J.S., 2002, MNRAS, 331, 795
- Miller L., Peacock J.A., Mead A.R.G., 1990, MNRAS, 244, 207
- Miyaji T., Hasinger G., Schmidt M., 2000, A&A, 353, 25
- Padovani P., Urry C.M., 1992, ApJ, 387, 449
- Padovani P., 1993, MNRAS, 263, 461
- Peacock J.A., 1985, MNRAS, 217, 601
- Press W.H., Teukolsky S.A., Vetterling W.T., Flannery B.P., 1992, Numerical Recipes, Cambridge Univ. Press, Cambridge
- Schmidt M., 1968, ApJ, 151, 393
- Shaver P.A., Wall J.V., Kellermann K.I., Jackson C.A., Hawkins M.R.S., 1996, Nature, 384, 439
- Shaver P.A., Windhorst R.A., Madau P., de Bruyn A.G., 1999, A&A, 345, 380
- Ueda Y., Akiyama M., Ohta K., Miyaji T., 2003, ApJ, 598, 886
- Urry C.M., Padovani P., 1995, PASP, 107, 803
- Vigotti M., Carballo R., Benn C.R., De Zotti G., Fanti R., Gonzalez Serrano J.I., Mack K-H, Holt J., 2003, ApJ, 591, 43
- Voges W., et al., 1999, A&A, 349, 389
- Voges W., Henry J.P., Briel U., Bräuninger H., Mullis C.R., Gioia I.M., Huchra J.P., 2001, ApJ, 553, 119
- Wall J.V., Peacock J.A., 1985, MNRAS, 216, 173
- Willott C.J., Rawlings S., Blundell K.M., Lacy M., 1998, MNRAS, 300, 625
- Willott C.J., Rawlings S., Blundell K.M., Lacy M., 1999, MNRAS, 309, 1017
- Willott C.J., Rawlings S., Blundell K.M., Lacy M., 2000, MNRAS, 316, 449
- Willott C.J., 2000, Conference proceeding "AGN in their cosmic environment", astro-ph/0007467
- Willott C.J., Rawlings S., Blundell K.M., Lacy M., Eales S.A., 2001, MNRAS, 322, 536